

Tori, disks, and winds — the first ten years of AGN interferometry

Sebastian F. Hönig

Abstract Infrared (IR) interferometry has made significant progress over the last 10 years to a level that active galactic nuclei (AGN) are now routine targets for long-baseline interferometers. Almost 50 different objects have been studied today in the near-IR and mid-IR. This allowed for detailed characterisation of the dusty environment of the actively growing black holes. It was possible to show directly that the dust must be arranged in clumps, as has been indirectly inferred from theory and unresolved observations. The dust composition seems to undergo significant evolution from galactic scales to the AGN environment, with the hottest dust close to the sublimation radius being dominated by large graphite grains. While the overall distribution of the dusty mass is quite diverse from object to object, indications have been found that the dust distribution may depend on AGN luminosity, with more powerful AGN potentially showing more compact dust structures. Arguably the most exciting discovery was the fact that the bulk of the mid-IR emission in Seyfert galaxies emerges from the polar region of the AGN, which is difficult to reconcile with classical torus models. An alternative model is currently being debated that consists of a dusty disk plus a dusty wind driven by radiation pressure from the central source. This finding has major implications for our understanding of AGN unification and will become a focus of the upcoming generation of instruments at the VLTI. More recently, an application of interferometry to cosmology was proposed to measure precise geometric distances to AGN in the Hubble flow. Further exploration of this method may open up interferometry to a new scientific community.

Sebastian F. Hönig
School of Physics & Astronomy, University of Southampton, Southampton, SO17 1BJ, United Kingdom, e-mail: S.Hoenig@soton.ac.uk

“After languishing for a decade largely through lack of data, this field should now see a revival, as it is refreshed by detailed infrared imaging. The dynamical problems guessed at years ago can be brought into clearer focus.”
— Julian Krolik, Nature News & Views, 2004

1 Active galactic nuclei 101

Every large galaxy in the universe hosts a supermassive black hole in its centre. Despite its enormous mass of several millions to billions of solar masses, it contributes typically less than 1% to the mass of the central bulges. Yet, the black hole mass is tightly correlated with at least the mass and velocity dispersion of the stars in the bulges. The question is: Why would the bulge care about the black hole? The common answer is that the growth phases and evolution of bulges and galaxies are interconnected via feeding and feedback mechanisms. These processes are particularly important in the active growing phases of the black holes, making active galactic nuclei (AGN) a central piece of the puzzle of how galaxies evolved over cosmic times.

The AGN phase is characterised as an episode of significant mass accretion, and number counts suggest that a supermassive black hole spends up to 10% of its lifetime as an AGN. The accreting mass forms a hot gas disk that emits radiation from the X-rays to optical wavelengths (see Fig. 1). Fast (> 1000 km/s) gas clouds orbit above and below the disk, giving rise to broad ultraviolet (UV) and optical emission lines (“Broad-line region”; BLR). At high elevation from the disk, highly ionised gas clouds are seen receding from the AGN, emitting narrow forbidden and permitted emission line (“Narrow-line region”; NLR). In the plane of the disk and at distances of > 0.1 pc away from the AGN, the temperature in the gas is cool enough for dust to survive. It is commonly pictured that this dusty, molecular gas forms a geometrically and optically thick torus, which obscures intersecting sight lines. At the same time, the absorbed UV and optical emission is re-radiated in the infrared. Such obscured AGN can only be identified by their IR emission and the narrow lines from high-ionised species from the NLR while the disk and broad lines are not visible. If we see the AGN unobscured, it is referred to as a “type 1” AGN; in the obscured case, we call it “type 2” (Antonucci, 1993). It should be noted that this picture is a gross simplification. Since the proposal of this geometric unification scheme in the 1980s, it has been realised that the degree of obscuration and the strength, broadness, and equivalent width of the various emission lines also depends on factors like specific accretion rate, environment, or evolutionary state. However, for the purpose of this review on AGN interferometry, we focus on galaxies that host “Seyfert” AGN – the garden variety class of AGN and poster child for the simple unification picture (barring controversial exceptions, of course).

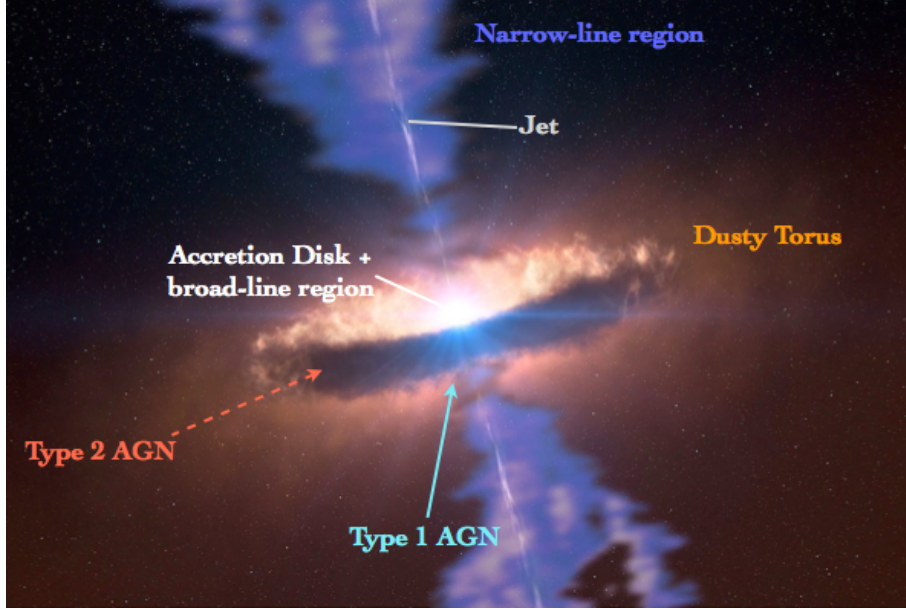


Fig. 1 Illustration of the mass distribution of the AGN phase. *Image: ESO, with modifications by the author.*

2 The dusty environment

The dusty region around the black hole plays an important role beyond obscuration. It is the most extended region that contributes to accretion, arguably connecting the black hole environment on sub-parsec scales to the host galaxy on scales of several tens to hundreds of parsec. Given its size it harbours a huge reservoir of gas that eventually feeds the black hole, making it a prime target of interest when trying to uncover interactions between black hole and galaxy that lead to coevolution. In addition, the infrared (IR) emission from the dust contributes a significant fraction to the overall radiative power output of the AGN.

As with the other structures of the AGN, the dusty region has typical angular sizes of few to several 10 milliarcseconds, which makes it impossible to directly resolve it with single telescopes. Therefore, most of what we know about the “torus” has been inferred indirectly. The basic framework we have is that the region must be dense enough to provide the obscuration seen in type 2 AGN. The spectral energy distribution (SED) in the IR suggests that dust temperatures range from about 200 K up to the sublimation temperature of ~ 1500 K, which leads to the expectation of the size range from sub-parsec to tens of parsec scales under the assumption of radiative equilibrium (Barvainis, 1987).

One important point has been inferred observationally and theoretically from a wide range of arguments (Krolik & Begelman, 1986, 1988; Tacconi et al., 1994):

The mass in the torus cannot be smoothly distributed but is rather arranged in clouds. These clouds have been described as cores or fragments of galactic molecular clouds, and must be very dense and compact. In order to withstand the shear of the gravitational potential of the black hole and be stable to its internal pressure, the clouds can only be as large as a small fraction of their distance from the AGN — typically less than 1%. In addition, their densities must be greater than about 10^8 cm^{-3} to be resistant against gas pressure and external forces (gravity and radiation pressure).

3 Infrared long-baseline interferometry of AGN: Pushing the limits

The biggest hurdle to test our picture of how mass accretion works for the supermassive black holes in the AGN phase are the small spatial scales involved. The accretion disk has a typical size of few light-days or less while the BLR reaches out to several light days in the Seyfert AGN. However, for objects with distances generally of the order of tens of Mpc, the angular sizes correspond to the sub-milliarcsecond scale. These scales are impossible to resolve with even the largest optical telescopes available or planned. The dusty region is our best shot since it extends out the furthest.

Within the last 10 years, infrared (IR) long-baseline interferometry has matured to a degree that we are now able to observe AGN. The major challenge in IR inter-

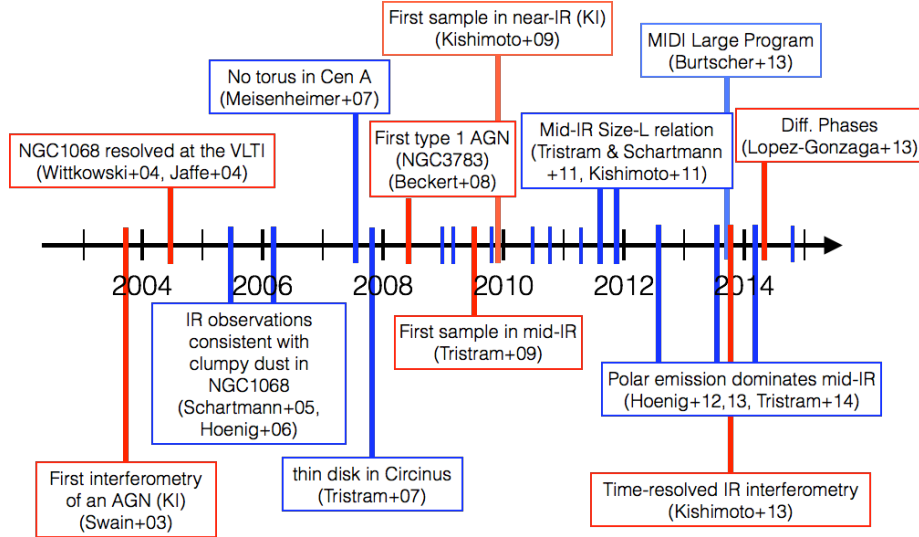


Fig. 2 Timeline showing the evolution of AGN publications from IR interferometry and its related interpretation/modelling. Several publications are highlighted based on a subjective selection by the author.

ferometry concerns the need to coherently combine the light “on the fly” in the presence of strong atmospheric disturbances of the signal, which influence the coherence strength and phase. The infrastructure involved in IR interferometry involves dozens of optical elements, reducing the overall transmission. This means that observations of AGN are usually sensitivity-limited. However, even under these circumstances, the persistent improvements on the two major large-telescope interferometers – the Very Large Telescope Interferometer (VLTI) on Paranal, and the Keck Interferometer (KI) on Mauna Kea – have led to AGN becoming routine targets, and the sample of objects is continuing to grow. While in the early 2000s, only the brightest sources NGC 4151 and NGC 1068 could be targeted (Swain et al., 2003; Wittkowski et al., 2004; Jaffe et al., 2004), we are now nearing a sample of 50 AGN that have been successfully observed in the near- or mid-IR (Tristram et al., 2007; Meisenheimer et al., 2007; Beckert et al., 2008; Raban et al., 2009; Kishimoto et al., 2009a; Burtscher et al., 2009; Tristram et al., 2009; Kishimoto et al., 2009b; Pott et al., 2010; Kishimoto et al., 2011a,b; Hönig et al., 2012, 2013; Burtscher et al., 2013; Tristram et al., 2014; López-Gonzaga et al., 2014), with some of them having both visibility (= centro-symmetric spatial information) and phase data (=non-symmetric spatial information). Furthermore, few objects are being monitored to study how their sizes evolve in the presence of variable central illumination (Pott et al., 2010; Kishimoto et al., 2013).

4 Science results

Fig. 2 shows a timeline of interferometry papers on AGN. Some key results¹ are highlighted that will be discussed in more detail in the following.

4.1 Sizes and what they mean

At the current stage of long-baseline interferometry, the main observable that can be used for scientific exploitation is visibility. Technically, visibility is the absolute value of the Fourier transform of the intensity distribution of an object, but for the purpose of AGN² we can consider it as the fraction of unresolved emission (or correlated flux) at a given baseline and position angle as compared to the single-telescope aperture of our total flux. Most of the time, we observe few combinations of baseline and position angle, which makes it impossible to properly reconstruct a full 2-dimensional brightness distribution. Therefore, we have to invoke models for the

¹ The label “key results” is a fully subjective judgment by the author of this chapter. They include the most cited papers in AGN IR interferometry

² where in all objects except of Circinus and maybe NGC 1068 we are observing in the first lobe of the Fourier transform

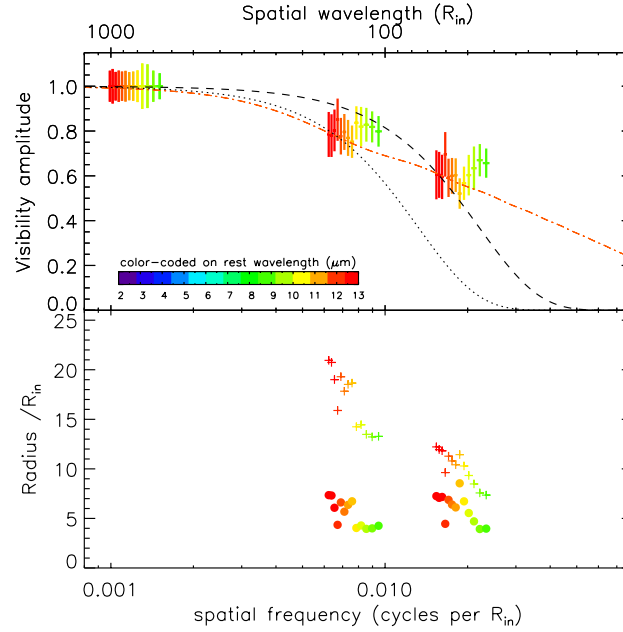


Fig. 3 Example for size extraction from visibilities (upper label) of three different baseline lengths using Gaussian models (black dotted and dashed lines) and a power-law (red dash-dotted line). While the power law is able to reproduce all data sets simultaneously, providing a unique size (see lower panel), the Gaussian model sizes depend on baseline length. From Kishimoto et al. (2011b).

brightness distribution based on which we can infer a size. That is: Interferometry does not measure a size; rather the size is inferred from visibility.

Since 2004, four different models have been used to turn AGN visibilities into sizes, which are more accessible to non-interferometrists.

- **Gaussian brightness distribution and FWHM size.** The beauty of the Gaussian function is its behaviour under Fourier transformation: it remains a Gaussian. Therefore early results used this function and reported the FWHM as inferred size of the respective object. The major problem with this model is that with better and more data available it became clear that the IR intensity distribution is not a Gaussian. As illustrated in Kishimoto et al. (2011b), this leads to the inferred FWHM strongly dependent on the visibility level (see Fig 3), so that the sizes are essentially representing λ /baseline rather than the object. Moreover, the better data required more than just one Gaussian to be employed for reproducing the brightness distribution.
- **Power-law brightness distribution and half-light radii.** Using the constraints from multi-baseline data, Kishimoto et al. (2009a) suggested a power law brightness distribution as the better representation. The corresponding size of such a distribution is the half-light radius (see Fig. 3). As shown in Kishimoto et al. (2011b), such a model results in almost no dependence of size on baseline in the

mid-IR data of six AGN. This should come as no surprise. The radiative transfer and dilution of light with distance from the AGN essentially set up a power law envelope. Even when convolved with a non-power-law mass distribution, power-law modes will remain, so that, in some sense, power laws may be considered a “natural brightness distribution” for the AGN IR emission. The major drawback of this model is that it requires sets of interferometric measurements at least at two different baseline lengths for any given position angle, which comes at the expense of significant observing time. However, angular and radial interpolation methods have been used to make use of measurements with offset position angles.

- **Point source plus Gaussian.** The AGN Large Programme (LP) performed with the mid-IR MIDI instrument at the VLTI seems to show many objects where the visibility dropped with baseline initially but then apparently flattens. Thus, Burtscher et al. (2013) took the approach to model the sources with a two-component model of a Gaussian plus a point source, the latter being responsible for the flattening. While one may argue that the Gaussian part introduces similar problems than with a single Gaussian (see above), the LP took the advantage of the large dataset for each individual object, modelled the distribution in 2D, and inferred half-light radii from these models. However, these half-light radii are different from the ones inferred from power laws and a proper comparison as to how they compare and how a power law brightness distribution fares for the LP sources is still pending.
- **Ring (plus point source).** Near-IR interferometry probes only the hottest dust near the sublimation radius. No dust emission emerges from closer than the sublimation radius. Therefore, it became a standard to use a thin ring model to infer sizes from near-IR interferometry (Kishimoto et al., 2007, 2009b, 2011a). Actually, the near-IR emission has significant contribution from the accretion disk – or “big blue bump” – of the order of a few to 25% depending on object. This skews the visibilities of the dust emission to higher values since the big-blue bump emission is much smaller and unresolved with current interferometers. Therefore, it is practical to combine a ring model with a point source, for which the contribution has been determined from spectral decomposition using optical to near-IR photometry.

For non-interferometrists it is important to remember that these sizes are model specific. They refer to a characteristic level to which the flux has been resolved, which could be 50% or any other “isophote”. As such, significant flux is present at larger radii than these size estimates, which is important to remember when making comparisons to models. Moreover, these sizes are wavelength-dependent and will typically increase with wavelength since cooler dust at larger distances from the AGN will contribute to the emission.

4.2 The dust is clumpy, indeed!

The first long-baseline IR interferometry was recorded with the KI in 2003 in the near-IR K -band of the brightest type 1 AGN NGC 4151 (Swain et al., 2003). The near-IR is supposed to trace the hottest dust close to being sublimated. However, the size of the inferred sublimation radius was smaller than expected, so the authors remained cautious on interpreting their result either as the ring of hot dust at the inner edge of the torus or gas emission from the allegedly much smaller accretion disk.

In 2004, the VLTI achieved its first fringes of an AGN in both the near- and mid-IR using the VINCI and MIDI instruments, respectively (Wittkowski et al., 2004; Jaffe et al., 2004). The target for both observations was NGC 1068, which is widely considered a prototype of local AGN. It is important to note that the MIDI instrument does not only provide single wavelength data, but covers the full 8 to 13 μm range – an interferometric IFU in some sense.

With the combination of these data, it could be shown that the wavelength-dependent size is consistent with dust in local thermal equilibrium with the AGN and confirmed that the IR emission is really from dust, something that has sometimes been questioned in literature given the comparably flat IR SEDs. Furthermore, with the aid of two sets of models (Schartmann et al., 2005; Hönig et al., 2006), it was possible to demonstrate that the fluxes at different spatial resolution elements is not consistent with a smooth distribution of dust, but requires the dust to be clumpy. This result was subsequently confirmed by observation of another nearby AGN, where the interferometric fluxes for a given baseline wiggled with position angle of the source (see Fig. 4) that can be only explained if the source is inhomogeneous (Tristram et al., 2007). These results were a first direct confirmation of substructure within the dusty gas and resoundingly confirmed theoretical predictions from more than a decade earlier.

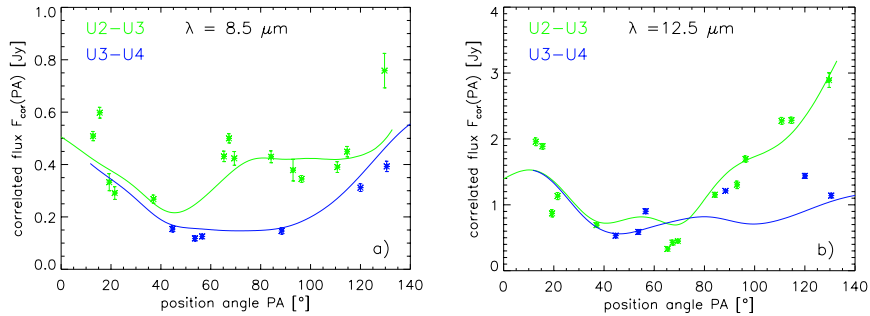


Fig. 4 “Wiggling” of the visibility at 8.5 μm (left) and 12.5 μm (right) for position-angle scans at two different fixed baseline lengths in the Circinus galaxy. Figure from Tristram et al. (2007).

Fig. 5 Sublimation radius inferred from near-IR interferometry with the KI (blue data points) as well as near-IR reverberation mapping (grey crosses). The dotted line shows a dependence of radius on the square root of the luminosity as expected from the Stefan-Boltzmann law. The normalisation is consistent with large graphite grain opacities. Figure from Kishimoto et al. (2011a).

over with only the tip of the original ISM dust distribution. Moreover, since silicate grains are supposed to sublime at lower temperatures than graphite, it is perfectly reasonable that the hottest dust is dominated by the latter type of grains.

These results should be put in light of the bigger picture. It has been noted that silicate emission features are lacking strength in observed mid-IR spectra of AGN while they feature prominently in any kind of dust torus model. Indeed, at interferometric resolution, silicate emission features are notably absent in spatially-resolved spectra of the inner few parsec of type 1 AGN (Beckert et al., 2008; Tristram et al., 2009; Burtscher et al., 2009; Kishimoto et al., 2011b; Burtscher et al., 2013). On the other hand, silicate absorption features, which indicate rather cool dust, are present in obscured type 2 AGN, albeit generally being rather weak. In addition, the strongest absorption features are probably not associated with the obscuring material in the nuclear environment, but originate from galactic scale extinction, e.g. from host dust lanes (Goulding et al., 2012; Hönig et al., 2014a). Putting these pieces together, the interferometry results are a strong indication of significant evolution of the dust composition with distance from the AGN.

4.4 Constraints on the volume filling factor

The dust size measurements lead to another interesting constraint: By relating the sizes to the flux emitted from this same region, we can calculate surface emissivities. Kishimoto et al. (2011b) assume that the typical hot dust temperature is 1400 K as inferred from spectral fits (Kishimoto et al., 2007). A black body emission model for the inferred interferometric half-light radius is then compared to the correlated flux from this radius (see Fig. 6).

For the hot dust emission near the sublimation radius, the inferred surface emissivity turns out to be ~ 0.3 in the six objects investigated by Kishimoto et al. (2011b). The interesting constraint we get from this comes from the fact that surface emissivity is the product of dust emissivity and surface filling factor. If this product is of the order 0.1, and considering that both individual factors must be smaller than approximately unity³, both factors are quite strictly limited to > 0.1 . For the dust emissivity, this is further evidence for the domination of large grains. The surface filling factor, on the other hand, is surprising, since it firmly limits the volume filling factor of the region to approximately $> (0.1)^{3/2} \sim 0.03$. This value still allows for clumpiness, but it might rule out low-volume filling factor models, as has been put forward in literature.

³ Strictly speaking, the brightness temperature inferred from spectral fits is a lower limit to the physical temperature, given the uncertainty from the dust distribution, which may make the emission appear redder than the temperature in this region. However, this effect should be minor at the inner rim of the dust distribution. If we assume that the “true” temperature is 1800 K, we can expect that the maximum value the emissivity can get to is ~ 3 for the assumption of a 1400 K black body. Similarly, The surface covering factor may be > 1 if the dust is optically thin. However, for the near-IR this is incompatible with the red SED towards the mid-IR, for which we would expect a Rayleigh-Jeans behaviour if optically thin.

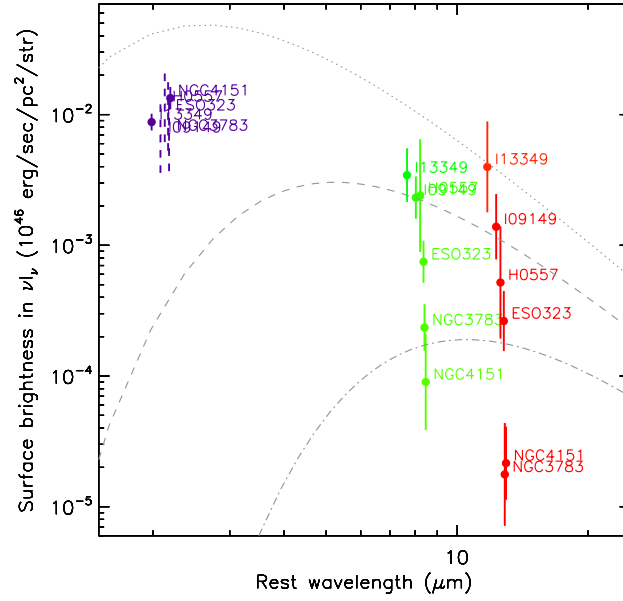


Fig. 6 Comparison of the observed surface brightness in the near-IR (violet) and mid-IR (green: 8 μm ; red: 13 μm) for the six AGN in Kishimoto et al. (2011b). The grey lines are black bodies with temperatures of 1400 K (dotted), 700 K (dashed) and 350 K (dash-dotted). See text for further information. Figure from Kishimoto et al. (2011b).

The situation is not as clear in the mid-IR. At these wavelengths, the emission is a mix of contributions from the Rayleigh-Jeans tail of hotter dust closer to the AGN and the “black body peaks” of cooler dust. Therefore, it is much more difficult to infer a representative temperature for the size measured with interferometry. Kishimoto et al. (2011b) compare the surface brightnesses of 700 K and 350 K black body emission to the resolved 8 and 13 μm emission from the half-light radii of their six AGN (see Fig. 6). A rather conservative lower limit can be set to the surface emissivity as > 0.01 , but given the uncertainties in the distribution of the dust, this result should be considered tentative.

In summary, IR interferometry indicates that clumpiness in the inner part of the dust distribution must be considered of the type with volume filling factor > 0.01 . With a better mapping of the dust emission using upcoming interferometric instrumentation, it will become possible to put a similar constraint on the cooler dust in the mid-IR that emits most of the energy in the IR.

4.5 The distribution of the dust revealed, but not clear what it means

One of the key features of IR interferometry is that it spans a rather large range of wavelengths. Aside from broadly covering the near- and mid-IR, structural information can be gathered with spectral resolution between 8 to 13 μm with the VLT/MIDI instrument. Translated into temperatures, we cover about 270 K to 450 K in νF_ν black-body equivalent. If all temperatures contributed equally, we could expect a difference in size from the shortest to longest wavelength in this window of a factor of 3–4 based on a modified Stefan-Boltzmann law for dust. In reality, however, the dust will not be distributed homogeneously but according to some mass density distribution, which can be considered a distance-depending weighting function for the temperature distribution. Using these simple considerations, and confirming it by full radiative transfer simulations (Hönig & Kishimoto, 2010), we can come up with the prediction that if the emission is emerging from a compact dust distribution close to the sublimation radius, then the size should not depend too much on wavelength, since the emission is dominated by a small range of hotter temperatures. Conversely, if the dust distribution is shallow, we expect a strong dependence on wavelength as more and more cooler dust at larger distances will contribute to the emission. This will effectively tie the shape of the total IR SED to the wavelength-dependent sizes, with blue SEDs coming from more com-

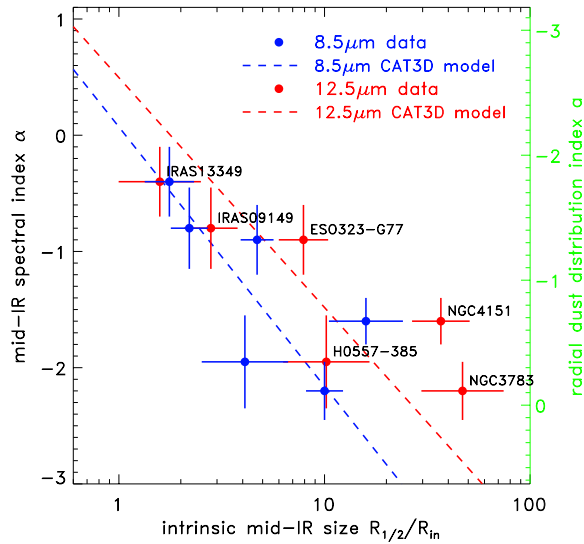


Fig. 7 Relation between the observed mid-IR spectral slope (expressed as a power law index) and the 8 μm (blue) and 13 μm (red) of the type 1 AGN sample in Kishimoto et al. (2011b). The dashed lines show the relation based on the *CAT3D* radiative transfer model Hönig & Kishimoto (2010) for which the radial dust distribution index was changed (green scale on the right y-axis).

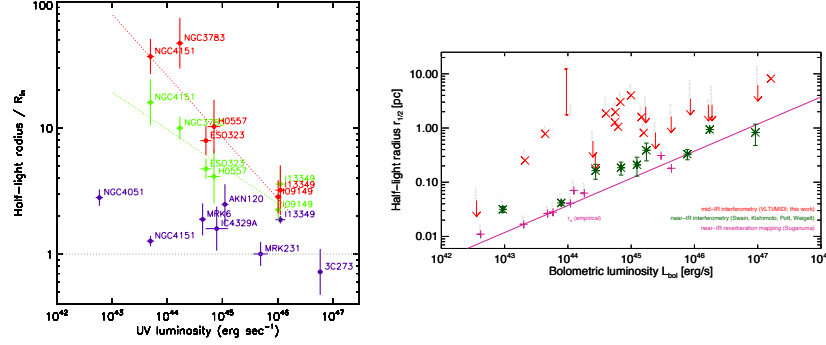


Fig. 8 *Left:* Mid-IR half-light radius in units of the inner radius of the dust distribution compared with the luminosity of the six AGN in Kishimoto et al. (2011b). The dust distribution becomes more compact at higher luminosity. *Right:* Near-IR and mid-IR sizes of objects in the MIDI Large Program plotted against AGN luminosity from Burtcher et al. (2013). A similar trend may be inferred, though at much higher scatter. Figures from Kishimoto et al. (2011b) and Burtcher et al. (2013).

pact and, thus, smaller distributions, while redder emission originates from more extended distributions (barring obscuration effects) Hönic & Kishimoto (2010).

To test this theoretical relation with observations, we have to remember that the absolute size of the inner boundary of the dust distribution (= sublimation radius) depends on the AGN luminosity. If we want to test the temperature distribution, and in turn the projected mass distribution, we are interested primarily in how the mass is distributed with respect to this inner boundary. Therefore, the absolute sizes we obtain from interferometry should be expressed in units of this inner scaling radius, which can be either inferred from near-IR interferometry or reverberation mapping. Taking this into account, we can indeed identify a dependence of (scaled) mid-IR size on the emission properties of the overall SED. When plotting the mid-IR half-light radii of the type 1 AGN in Kishimoto et al. (2011b) against the spectral slope in the IR, we find a quite strong dependence of both parameters (see Fig. 7). This backs the idea that the wavelength-dependence of the interferometric sizes traces the (projected) distribution of the dust mass (Hönic et al., 2010).

A more puzzling relation is found when comparing the compactness of the dust emission with AGN luminosity. Kishimoto et al. (2011b) found for their sample of 6 unobscured AGN that the brightness distribution becomes more compact with luminosity (see Fig. 8 left). On the luminous end ($\sim 10^{46} \text{ erg/s}$), the mid-IR emission seems to be almost entirely emerging from the Wien tail of hot dust in the vicinity of the sublimation radius, while on the lower luminosity side ($\sim 10^{43} \text{ erg/s}$) the hot dust is extended beyond 50 times the sublimation radius. Indications of such a trend may also be identified in the type 1s of the more expansive MIDI LP dataset Burtcher et al. (2013), although the picture is messier there (see Fig. 8 right). The major problem at this point is the limited number of sources at higher luminosities. If we assume, however, that the trend is real, we have yet to find a physical model to

explain it. Note that this “compact when luminous” trend is distinct from the ideas of a receding torus (Lawrence, 1991; Simpson, 2005), which has been considered for the effect that higher luminosity AGN might have lower dust covering factors: The receding torus may account for a *vertical* evolution with luminosity, but it does not necessarily require a *radial* evolution of the mass distribution in units of the sublimation radius.

4.6 Where is the torus after all?

Arguably the most challenging result for our understanding of AGN from IR interferometry comes from detailed observations of the four galaxies NGC 1068 (Raban et al., 2009), NGC 424 Hönig et al. (2012), NGC 3783 Hönig et al. (2013), and Circinus Tristram et al. (2014). The mid-IR brightness distribution in each of these sources is mapped with 40 or more individual data points scattered from few 10 m up to 130 m baseline lengths and at all position angles that can be reached with the VLTI. This unprecedented level of detail allowed for precise analysis of the position-angle dependence of the emission source. Surprisingly, all four sources displayed strong elongation in the polar direction of the AGN, i.e. *perpendicular* to the plane of the torus (see Fig. 9). While one may argue that radiative transfer and obscuration effects play a role in this appearance for the three type 2 sources, this argument becomes less compelling for NGC 3783, which is a type 1 AGN. Moreover, the elongations in polar direction are substantial, with inferred axis ratios of 3–4. Finally, the emission originating from these polar features dominates the total

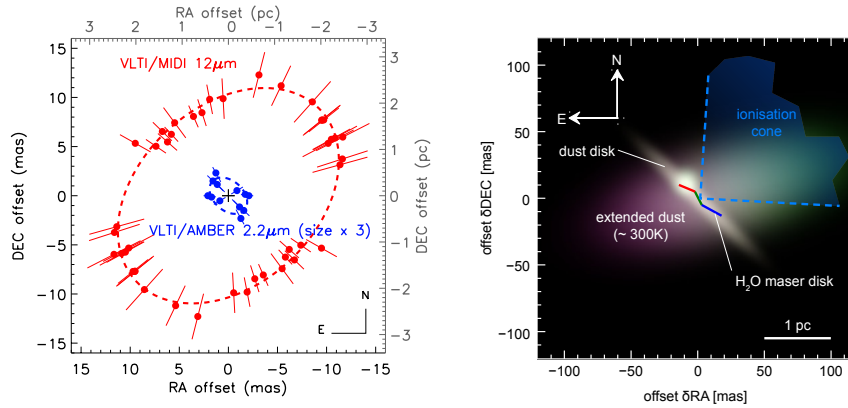


Fig. 9 *Left:* Position-angle dependent sizes of the near-IR (blue) and mid-IR (red) emission in NGC 3783 as observed with VLT/AMBER and VLT/MIDI. The mid-IR ellipse is elongated toward the polar region while the near-IR emission is aligned with the plane of the AGN (Hönig et al., 2013). *Right:* Model image of the dusty environment in the Circinus galaxy based on the mid-IR interferometry data from Tristram et al. (2014). See text for further description.

mid-IR emission in all four sources. Such extreme polar features, in particular in a type 1 source, are very difficult to reconcile with a classical torus model.

NGC 3783 was also the target of the first successful AGN observations with VLTI/AMBER (Weigelt et al., 2012). A preliminary analysis of the position angle dependence suggests that the hot dust emission as traced by these near-IR interferometry observations is aligned with the equatorial plane where models would locate the torus, i.e. probably perpendicular to the observed mid-IR emission (Hönig et al., 2013). The covering factor of this near-IR disk has been constrained to $\sim 30\%$. Similarly in Circinus, on top of the 80% of mid-IR flux emerging from the polar region, the bulk of the remaining flux has been found to be in a geometrically thin disk aligned with known maser emission (Tristram et al., 2014). However, the scale height over most of this disk’s extension is substantially smaller than what torus models require.

These two observations suggest that the dusty environment constitutes of two separate entities: (1) a geometrically thin disk in the equatorial plane of the AGN, potentially dominating the near-IR fluxes, and (2) a strong polar component dominating the overall mid-IR emission. It has been suggested that this polar component represents a dusty wind which is launched from near the inner region of the disk by the string radiation pressure on dust (Hönig et al., 2012). Indeed, radiation-hydrodynamical models suggest that such flows can exist (Wada, 2012; Dorodnitsyn et al., 2012; Schartmann et al., 2014), but further theoretical and observational work is required to solidify these ideas.

Notwithstanding the final theoretical assessments of the physical origin, these observations strongly suggest that our original idea of a simple torus has to be thrown overboard. The two-component structure offers important new constraints on what models have to reproduce to explain the mass distribution around AGN. Beyond the impact on unification, if the polar emission does indeed originate from a dusty wind, it may be connected to the much larger kpc scale molecular winds that are invoked as a feedback mechanism of AGN onto the galaxy. At least in NGC 1068 and Circinus, we do see that the mid-IR emission extends much beyond interferometric scales and can be traced to at least 100 pc in single-telescope images. This indicated that IR interferometry observes the region of origin of AGN feedback. ALMA may help us making this connection more directly by simultaneously tracing the molecular component of dust clouds at IR interferometry resolution and larger regions.

5 Conclusions and outlook

IR interferometry has contributed a unique view into the mass distribution around supermassive black holes. It allowed us to access small spatial scales that are out of reach for any single telescope, even for the upcoming generation of extremely large telescopes. The two key messages to keep in mind are as follows:

- While in the beginning only the few brightest targets were observable, we are now closing in on 50 different AGN with constraints from interferometry. A

whole suite of data sets is available now in the near-IR and mid-IR, ranging from visibilities to differential and closure phases and monitoring information.

- With the help of spectrally resolved interferometry, it was possible to map the dust brightness distribution around AGN. The dust seems to be clumpy with a volume filling factor of the order $0.01 - 0.1$. The dust undergoes significant evolution in the AGN environment under the influence of the strong, hard radiation field. Finally the dust distribution among the whole AGN sample looks quite diverse, but there are indications of a trend of more compact distributions for higher luminosity AGN. This is yet to be confirmed, however.
- Most surprisingly, the bulk of the pc-scale mid-IR emission in AGN seems to originate from the polar region of the AGN, not from the equatorial plane where the torus is located. A new two-component picture is emerging consisting of a dense dusty disk, in the plane of accretion onto the AGN, and an extended polar wind, where dusty gas is pushed out by the strong radiation pressure from the AGN.

The polar extended emission will become a major field of research for AGN interferometry in the coming years with the new MATISSE (mid-IR) and GRAVITY (near-IR) instruments going online at the VLTI. These instruments will combine all four UT telescopes and enable us to create real images from AGN interferometry data for the first time. MATISSE will also add new capabilities as $3.6\ \mu\text{m}$ and $4.5\ \mu\text{m}$, which are sweet spots for AGN research. We now have an unprecedented opportunity to pin down the mass distribution around AGN in the dust and gas phase by making use of the high-angular resolution facilities that ESO has to offer in the IR (VLTI) and sub-mm (ALMA).

Another interesting new path for the VLTI was recently suggested (Hönig et al., 2014b). By combining near-IR interferometry with reverberation mapping, it is possible to use simple trigonometric principles to measure precise direct distances to AGN (see Fig. 10). As described above, the hot dust around an AGN essentially forms a narrow ring. With near-IR interferometry, we can determine the angular size of this ring. Near-IR reverberation mapping measures the time lag between variability seen in the visual and its dust-reprocessed version in the near-IR. Since the visual light originates from the putative accretion disk, which is at least an order of magnitude smaller than the hot dust ring, the time lag can be converted into a physical size, which corresponds to the physical radius of the hot dust ring. The distance can then be calculated from the ratio of the angular and physical size.

This new “dust parallax” method, being a spin-off of an earlier suggestion for line emission (Elvis & Karovska, 2002), has been showcased for NGC 4151. The distance was determined as $19.0^{+2.4}_{-2.6}$ Mpc, which means that the combined systematical and statistical errors are of the order of $12 - 13\%$. If this precision can be held up for other objects, it will be a competitive method for cosmological applications. The systematical uncertainties are dominated by the geometry of the brightness distribution, such as its inclination and orientation, which can be well constrained with the help of the new VLTI instruments. They allow for a better mapping of the near-IR emission source, including phase information to probe asymmetries.

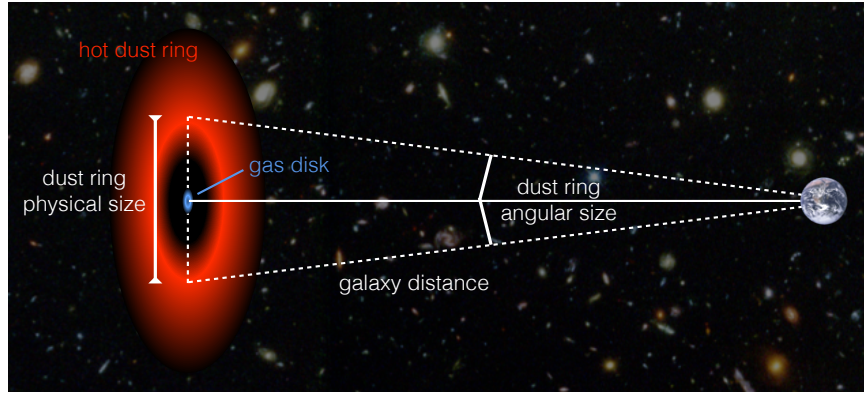


Fig. 10 Illustration of the “dust parallax” method to determine geometric distances to AGN (Hönig et al., 2014b). While interferometry measures the angular size of the hot dust ring, its physical size can be inferred from reverberation mapping (see text for details).

One interesting aspect is the possibility to measure geometric distances directly in the Hubble flow at > 100 Mpc. Indeed, dozens of AGN with a K-band magnitude between 10.5 and 12 would be suitable for this exercise. If reached with interferometry, we could independently estimate the Hubble constant without invoking the many steps in the cosmological distance ladder and address the current tension between local measurements and inferences from the Cosmic Microwave Background. Therefore, it may be worth considering to put some additional efforts into increased sensitivity of interferometric instrumentation in the near-IR.

“The most impressive recent results [on AGN unification] are due to IR interferometry. Long baseline interferometry is the way of the future.”
— Hagai Netzer, *Annual Review of Astronomy & Astrophysics*, 2015

References

- Antonucci, R. 1993, *ARA&A*, 31, 473
Barvainis, R. 1987, *ApJ*, 320, 537
Beckert, T., Driebe, T., Hönig, S. F., & Weigelt, G. 2008, *A&A*, 486, L17
Burtscher, L., Jaffe, W., Raban, D., Meisenheimer, K., Tristram, K. R. W., & Röttgering, H. 2009, *A&A*, 705, L53
Burtscher, L., Meisenheimer, K., Tristram, K. R. W., et al. 2013, *A&A*, 558, 149
Dorodnitsyn, A., Kallman, T., & Bisnovatyi-Kogan, G. 2012, *ApJ*, 747, 8
Elvis, M., & Karovska, M. 2002, *ApJL*, 581, L67
Goulding, A. D., Alexander, D. M., Bauer, F. E., et al. 2012, *ApJ*, 755, 5
Hönig, S. F., Beckert, T., Ohnaka, K., & Weigelt, G. 2006, *A&A*, 452, 459
Hönig, S. F., Kishimoto, M., Gandhi, P., et al. 2010, *A&A*, 515, 23

- Hönig, S. F., & Kishimoto, M. 2010, *A&A*, 523, 27
- Hönig, S. F., Kishimoto, M., Antonucci, R., et al. 2012, *ApJ*, 755, 149
- Hönig, S. F., Kishimoto, M., Tristram, K. R. W., et al. 2013, *ApJ*, 771, 87
- Hönig, S. F., Gandhi, P., Asmus, D., Mushotzky, R. F., Antonucci, R., et al. 2014a, *MNRAS*, 438, 647
- Hönig, S. F., Watson, D., Kishimoto, M., & Hjorth, J. 2014b, *Nature*, 515, 528
- Jaffe, W., Meisenheimer, K., Röttgering, H. J. A., Leinert, Ch., Richichi, A., et al. 2004, *Nature*, 429, 47
- Kishimoto, M., Hönig, S. F., Beckert, T., & Weigelt, G. 2007, *A&A*, 476, 713
- Kishimoto, M., Hönig, S. F., Tristram, K., Weigelt, G. 2009, *A&A*, 493, L57
- Kishimoto, M., Hönig, S. F., Antonucci, R., et al. 2009, *A&A*, 507, L57
- Kishimoto, M., Hönig, S. F., Antonucci, R., et al. 2011a, *A&A*, 527, 121
- Kishimoto, M., Hönig, S. F., Antonucci, R., et al. 2011b, *A&A*, 536, 78
- Kishimoto, M., Hönig, S. F., Antonucci, R., Millan-Gabet, R., Barvainis, R., et al. 2013, *ApJL*, 775, L36
- Krolik, J. H., & Begelman, M. 1986, *ApJL*, 308, 55
- Krolik, J. H. & Begelman, M. C. 1988, *ApJ*, 329, 702
- Lawrence, A. 1991, *MNRAS*, 252, 586
- López-Gonzaga, N., Jaffe, W., Burtscher, L., Tristram, K. R. W., & Meisenheimer, K. 2014, *A&A*, 565, 71
- Meisenheimer, K., Tristram, K. R. W., Jaffe, W., Israel, F., Neumayer, N., et al. 2007, *A&A*, 471, 453
- Pott, J.-U., et al. 2010, *ApJ*, 715, 736
- Raban, D., Jaffe, W., Röttgering, H., Meisenheimer, K. & Tristram, K. R. W. 2009, *MNRAS*, 394, 1325
- Schartmann, M., Meisenheimer, K., Camenzind, M., Wolf, S., & Henning, T. 2005, *A&A*, 437, 861
- Schartmann, M., Wada, K., Prieto, M. A., Burkert, A., & Tristram, K. R. W. 2014, *MNRAS*, 445, 3878
- Simpson, C. 2005, *MNRAS*, 360, 565
- Suganuma, M., Yoshii, Y., Kobayashi, Y., Minezaki, T., Enya, K. et al. 2006, *ApJ*, 639, 46
- Swain, M., Vasisht, G., Akeson, R., Monnier, J., Millan-Gabet, R., et al. 2003, *ApJ*, 596, L163
- Tacconi, L. J., Genzel, R., Blietz, M., Cameron, M., Harris, A. I., & Madden, S. 1994, *ApJ*, 426, L77
- Tristram, K. R. W., Meisenheimer, K., Jaffe, W., Schartmann, M., Rix, H.-W., et al. 2007, *A&A*, 474, 837
- Tristram, K. R. W., Raban, D., Meisenheimer, K., Jaffe, W., Röttgering, H., et al. 2009, *A&A*, 502, 67
- Tristram, K. R. W., Burtscher, L., Jaffe, W., Meisenheimer, K., Hönig, S. F., et al. 2009, *A&A*, 502, 67
- Wada, K. 2012, *ApJ*, 758, 66
- Weigelt, G., Hofmann, K., Kishimoto, M., et al. 2012, *A&A*, 541, L9

Wittkowski, M., Kervella, P., Arsenault, R., Paresce, F., Beckert, T., & Weigelt, G.
2004, A&A, 418, L39